Memory and aging effects in interacting sub-10nm nanomagnets with large uniaxial anisotropy

Kai-Cheng Zhang and Bang-Gui Liu

Institute of Physics, Chinese Academy of Sciences, Beijing 100190, China and
Beijing National Laboratory for Condensed Matter Physics, Beijing 100190, China
(Dated: June 6, 2009)

Using a nonequilibrium Monte Carlo method suitable to nanomagnetism, we investigate representative systems of interacting sub-10nm grained nanomagnets with large uniaxial anisotropy. Various magnetization memory and aging effects are found in such systems. We explain these dynamical effects using the distributed relaxation times of the interacting nanomagnets due to their large anisotropy energies.

I. INTRODUCTION

Nanomagnets attract huge interest because of their amazing properties and promising applications[1, 2, 3, 4, 5, 6]. For well-separated nanomagnets (including single-molecule magnets), quantum tunnelling, interference, and coherence can be observed at extra-low temperatures[6, 7, 8, 9, 10], and the magnetization behaviours at some higher temperatures can be described by Neel-Brown law [11, 12]. When inter-particle distances become small enough, the dipolar-dipolar interaction will modify the magnetization behavior leading to some super-spin-glasses behaviors[13, 14], similar to conventional spin glasses [15, 16, 17, 18]. Grained nanomagnets with large *uniaxial* anisotropy are essential to modern magnetic data storage. For typical CoCrPtB media, usual average grain sizes must be about 10nm to keep magnetic stability of 10 years at room temperature[19]. In the case of CoCrPt-oxide media for perpendicular recording, dominant inter-grain interactions are weak antiferromagnetic (AFM) couplings and average grain size can be 8nm or smaller for the same stability[19]. Such average size can even be reduced down to 3nm or smaller when FePt in the L1$_0$ phase is used as data storage media, because its magnetocrystalline anisotropy reaches to 44 meV/nm^3[19]. Such nanomagnets with large uniaxial anisotropy, especially when composing special systems, can yield various dynamical phenomena waiting for exploration.

Here we explore dynamical magnetic properties of representative systems of sub-10nm grained nanomagnets with large uniaxial anisotropy. We use the giant spin approach for the nanomagnet because the magnetic interactions between electronic spins in it are strong. We assume that the magnetic anisotropy energies satisfy a Gaussian distribution to consider their fluctuations due to different shapes, sizes, and interfacial environments, and the inter-nanomagnet interactions, including magnetic dipolar interaction, are AFM[19]. We use a giant-spin model and a dynamical spin Monte Carlo (DSMC) method[20] to correctly simulate dynamical magnetization of the giant-spins of the component nanomagnets.

Through systematical DSMC simulations, we find various field-cooling (FC) and zero-field-cooling (ZFC) magnetization memory and aging effects in such systems. We explain these dynamical effects uniformly in terms of the continuously-distributed relaxation times of the component nanomagnets due to the various uniaxial anisotropy energies. More detailed results will be presented in the following.

II. MODEL, METHOD AND PARAMETERS

We consider a finite two-dimensional lattice of grained nanomagnets. Each nanomagnet actually includes many magnetic atoms, but the magnetic interactions between the magnetic atoms are much stronger than those among different nanomagnets. The inter-nanomagnet magnetic interactions are described by an antiferromagnetic coupling according to actual materials for modern magnetic data storage[19]. We take the giant spin approach and use one spin variable $\vec{S}_i$ to describe the magnetic property of each nanomagnet. Because the spin value S_i of such a nanomagnet is typically $10^2 \sim 10^3$, large anisotropy energies of such nanomagnets are mainly dependent on their shapes and interfacial environments[19], and thus can be reasonably assumed to satisfy a Gaussian distribution. This simplification keeps the main physics of these nanomagnet systems. Because S is large enough, we treat the spin operator $\vec{S}_i$ as $S_i\vec{s}_i$, where $\vec{s}_i$ is a classical unit vector. Generally speaking, S_i should vary from one nanomagnet to another, but for our systems all the $\{S_i\}$ are uniform enough to be let have the same average value $\bar{S}$ because the deviations from $\bar{S}$ make little differences. Therefore, our model can be described by the Hamiltonian,

$$H = -\sum_i k_{ui}\vec{s}_{iz}^2 + \sum_{i,j} J_{ij}\vec{s}_i \cdot \vec{s}_j - \gamma\vec{B} \cdot \sum_i \vec{s}_i \quad (1)$$

where k_{ui} describes the uniaxial anisotropy energy satisfying a Gaussian distribution with the average value k_u and width σ_u, γ is defined as $g\mu_0\mu_B\bar{S}$, and the field $\vec{B}$ is in the easy axis. Here J_{ij} describes the inter-nanomagnet AFM interactions. For actual perpendicular media for

modern magnetic data storage, we assume that the easy axis is perpendicular to the plane of the $N \times N$ nanomagnet lattice. In such a setup, the magnetic dipolar interaction is reduced to an AFM inter-nanomagnet interaction, which has been included in the J_{ij} parameters in Eq. (1).

Each of the spins has two meta-stable orientations along the easy axis and needs to overcome an energy barrier to achieve a reversal. We use the DSMC method to simulate the spin dynamics of these nanomagnet systems[20]. This method originates from the kinetic Monte Carlo method for simulating atomic dynamics during epitaxial growth[21]. Using θ_i to describe the angle deviation of $\vec{s}_i$ from the easy axis, we express the energy increment of the i-th nanomagnet as $\Delta E_i = k_{ui} \sin^2 \theta_i - h_i(\cos \theta_i - 1)$ to leading order, where $h_i = (\gamma B - \sum_j J_{ij} s_j) s_i$ and the reduced variable s_i takes either 1 or -1[20]. As a result, an energy barrier $\Delta E_i = (2k_{ui} + h_i)^2 / 4k_{ui}$ must be overcome to achieve the reversal of the i-th spin. The rate for the spin reversal obeys Arrhenius law $R_i = R_0 \exp(-\Delta E_i / k_B T)$, where k_B is Boltzmann constant and T is temperature.

In our simulation, we use a typical value $1.0 \times 10^9/s$ for the characteristic frequency R_0. As for the anisotropy energy parameters, we reasonably assume that the average value k_u of $\{k_{ui}\}$ is 80.0 meV and the Gaussian width σ_u is 44.7 meV. We change temperature T by a step 0.2 K and set the sweeping rate to 1 K/s in most of the following cases. Special cases will be explicitly described otherwise. We take $N = 40$ and use periodic boundary condition. This lattice size is appropriate considering the actual situation in the media for the modern magnetic data storage. It almost does not matter which boundary condition is chosen with the lattice size. Further simulations with larger N are done for confirmation. Each of our data is obtained by calculating the average value over 500~1000 independent simulation runs.

III. MAIN SIMULATED RESULTS

FC and ZFC magnetization curves. We simulate the FC curves by calculating the average magnetizations under 100 Oe at every T point when cooling from 110 to 10 K. The ZFC curves are simulated by letting the system cool under zero field from 110 to 10 K and then calculating the average magnetizations under 100 Oe at every T point when warming from 10 to 110 K. Our simulation realizes what happens in measuring experimental FC and ZFC magnetization curves. Our simulated results are presented in Figure 1. For zero interaction or $J = 0$, the FC magnetization increases monotonously with decreasing T, and the ZFC magnetization increases first with increasing T, reaches its maximum at the blocking temperature $T_B = 55$ K, and then decreases. The FC and ZFC magnetization curves follow the Curie law above the temperature $T_m = 70$ K. The difference between the FC and ZFC magnetizations diminishes above

T_m. Such behaviors are key features of nanomagnets, showing up in super-spin glass systems[13] and interacting nanoparticles[22, 23]. When J is larger, the magnetization in the FC and ZFC curves becomes substantially smaller, as shown in Figure 1. When J becomes further larger, a minimal magnetization can be seen below T_B. It is at 30 K for 2.0 meV. When J is less than 0, the magnetization in such curves becomes larger but the curve shape remains nearly the same.
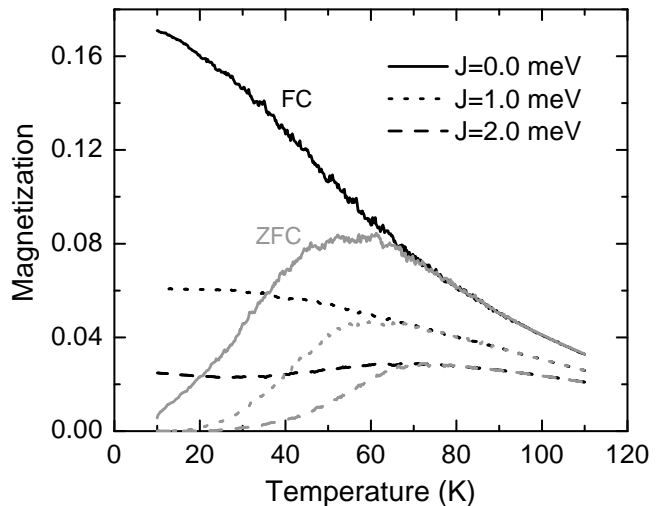

FIG. 1: Simulated FC (black) and ZFC (gray) magnetization curves under a field 100 Oe for $J = 0.0$, 1.0, and 2.0 meV. These curves are calculated in the same way as corresponding experimental magnetization curves are measured.

Simulated ZFC and FC memory effects over time. Cool the system under zero field to a low temperature, 30 K, and then apply a field 500 Oe and let the system relax from $t = 0$. At $t_1 = 814$ s, we change T to 10 K and reverse the field, and at $t_2 = 4124$s, we recover the original temperature and field. We calculate the average magnetization when the system relaxes with time from $t = 0$ to $t = 15000$s, and present the results in Figure 2a. The magnetization at t_2 is equivalent to that at t_1, that is, the system keeps the memory at t_1 although it undergoes relaxation from t_1 to t_2 under the different temperature and field. This is a ZFC memory effect over time. In addition, we cool the system under a field 500 Oe to 30 K, and then remove the field and let the system relax from $t = 0$, but we change the temperature to 10 K and the field to -500 Oe between $t'_1 = 3416$s and $t'_2 = 6730$s. Meanwhile we calculate the magnetization from $t = 0$ to $t = 20000$s. The result, shown in Figure 2b, shows an FC memory effect over time, $m_{t'_2} = m_{t'_1}$. Similar effect was observed in super-spin glass systems and interacting nanoparticles[14, 22, 23]. Our further calculations show that a small inter-spin interaction, either AFM or FM, does not affect the effects substantially.

Simulated FC memory effect over temperature. Cool the system under a field 100 Oe from 110 to 10 K, but
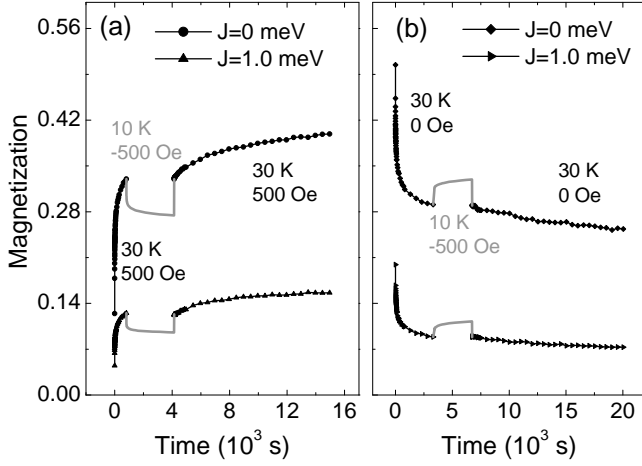
FIG. 2: Simulated ZFC (a) and FC (b) memory effects over time with $J = 0$ and 1.0 meV. (a) The temperature is 30 K and the field 500 Oe at all the time points except between $t_1 = 814$ s and $t_2 = 4129$ s (gray); in the special time period, the temperature and field are changed to 10 K and -500 Oe. (b) The temperature is 30 K and the field 0 Oe at all the time points except between $t'_1 = 3416$ s and $t'_2 = 6730$ s (gray); in the special time period, the temperature and field are changed to 10 K and -500 Oe.
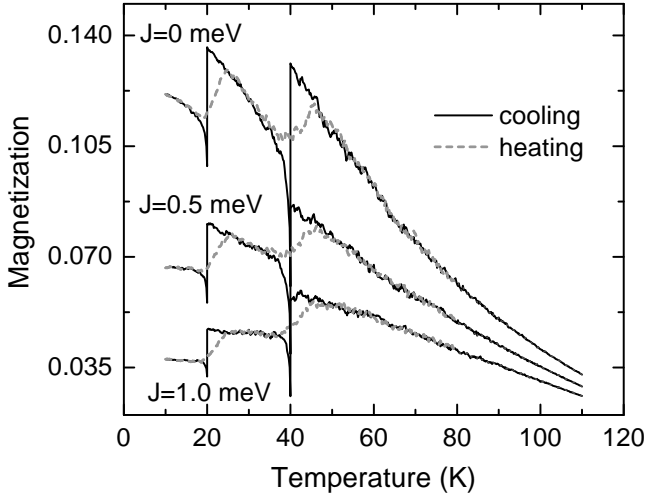

FIG. 3: Simulated FC memory effects over temperature for $J = 0.0$, 1.0, and 2.0 meV. During cooling (black), the temperature is changed homogeneously and the field is 100 Oe at all the temperature points except 40 K and 20 K. At these two special temperature points, the system is kept at the temperature for additional 40 s and 60 s, respectively, and the field is kept constantly the same -100 Oe meanwhile. The heating (gray dash) is homogeneous in time under the same field.

at two temperature points, 40 K and 20 K, the field is reversed and then recovers after 40 s and 60 s, respectively. The resulting FC magnetization curves for $J = 0$, 0.5, and 1 meV are shown in Figure 3. The step is clearly seen at both 40 K and 20 K for each of the three curves.
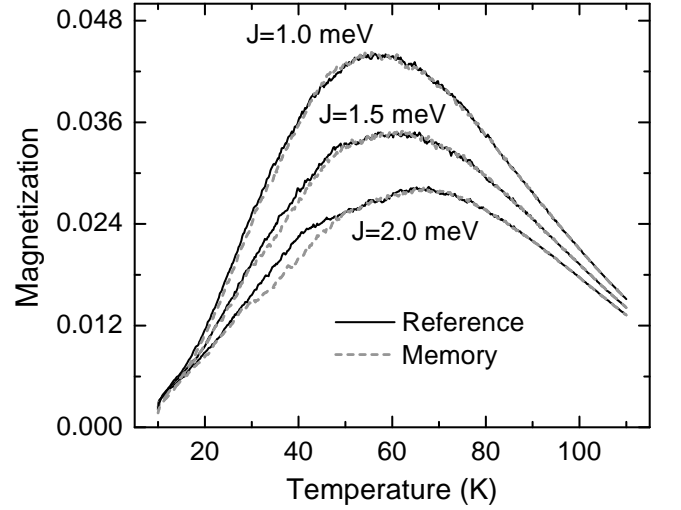

FIG. 4: Simulated ZFC memory effects over temperature for $J = 1.0$, 1.5, and 2.0 meV. The references (black lines) are standard ZFC magnetization curves with 100 Oe, and the memory curves (gray dash lines) are made by keeping the system relaxing for additional 100 s at 40 K during the cooling. The heating is always homogeneous in time and field.

The abrupt magnetization change is because the field is kept as the reversed value, -100 Oe, for additional 40 s or 60 s. When the cooling ends at 10 K, we warm the system under 100 Oe from 10 to 110 K. The corresponding three warming magnetization curves are presented in Figure 3. Clear magnetization drop is observed at both 40 K and 20 K, although the warming is homogeneous in time and field. This means that the system during the warming has the memory of the abrupt magnetization changes at the same temperatures during the cooling. Similar effects have been observed in interacting nanoscale systems[14, 22, 23]. Our results show that a small inter-spin interaction changes the FC memory effect only a little.

Simulated ZFC memory effect over temperature. The above effects are essentially independent of inter-spin interactions J. Such interactions weaken, even can break these memory effects, but appropriate J values can lead to another memory effect shown in Figure 4. First, cool the system homogeneously under zero field, calculate standard ZFC magnetization curves when warming the system under 100 Oe, and take them as references; then, cool the system under zero field but keep it for additional 100s when $T = 40$ K, calculate corresponding magnetization curves when warming the system under 100 Oe. Although the warming is homogeneous in time, the magnetization near 40 K is smaller, which implies that the system has the memory of the waiting at 40 K during the cooling. These are consistent with observations in the cases of other interacting super-spin systems[24, 25]. It is clear that nonzero J values are helpful for the memory effect.
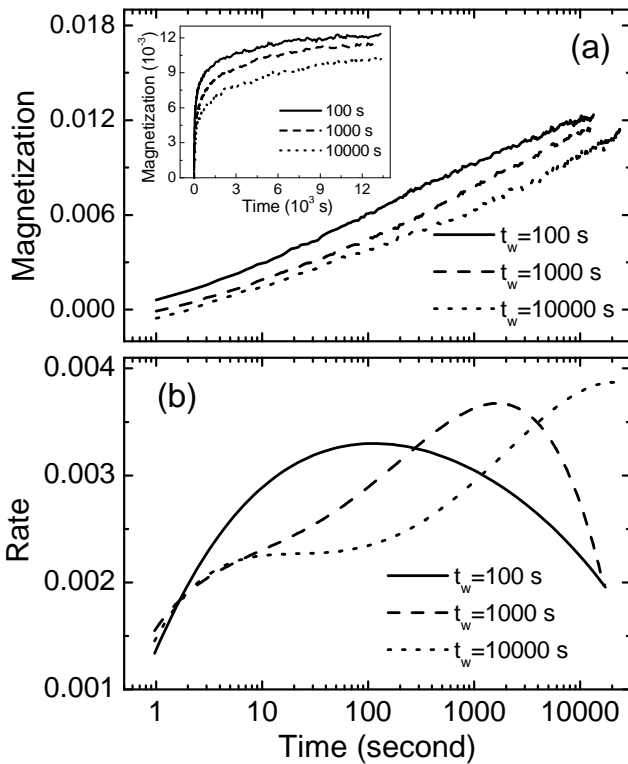
FIG. 5: Simulated aging effect. The magnetization m (a) and rate S (b) as functions of time t at 15 K under 100 Oe for three waiting time periods t_w: 100s (solid), 1000s (dash), and 10000s (dot). The inset in (a) shows the same m results in the linear scale of t.

Simulated aging effect. Cool the system under zero field to 15 K (below T_B) and keep it unchanged for a period t_w, and then let it relax with time t under 100 Oe. During the relaxation, we calculate the magnetization m and the rate $S = \partial m / \partial \log t$ as functions of t. Our simulated results in logarithmic scale with $t_w = 100$s, $t_w = 1000$s, and $t_w = 10000$s are presented in Figure 5. The inset in the upper panel shows the magnetization in linear scale of t. It is clear that the longer the waiting time, the smaller the magnetization, and the relaxation rate has a maximum at $t \approx t_w$. This is consistent with well-known aging effect observed in spin-glass and inter-acting super-spin systems[13, 15, 24, 25].

IV. DYNAMICAL MECHANISM AND COMPARISON WITH EXPERIMENT

Mechanism for the memory and aging effects. Our systems consist of nanomagnets with large uniaxial magnetic anisotropy which follows Gaussian distribution. The distribution of anisotropy energy causes various relaxation times through relation $\tau_i = \tau_0 \exp(\Delta E_i / k_B T)$. The memory and aging effects can be explained in a unified way by the continuously-distributed relaxation times $\{\tau_i\}$

of nanomagnets. The key point is that for a given time period and at a given temperature, most effectively re-laxed are the nanomagnets with appropriate relaxation time τ because those with smaller τ have been sufficiently relaxed and those with larger τ remain frozen. For the memory effects over time shown in Figure 2, the temperature between the two time points, t_1 and t_2 (or t'_1 and t'_2), is substantially lower, and nothing important happens meanwhile, although the field is changed, because the nanomagnets with much smaller τ have already been thoroughly relaxed, and hence the magnetization is re-covered after the field and temperature are restored. As for the memory effect shown in Figure 3, the additional relaxation under the reversed field at both 40 K and 20 K during the cooling makes corresponding nanomagnets orient in the reversed direction and most of them, re-maining frozen at the lower temperatures in the further cooling, cause the magnetization dips at both 20 K and 40 K in the warming curve, the FC memory effect over temperature. For the ZFC memory effect shown in Fig-ure 4, the additional 100 s relaxation at 40 K during the cooling, in the presence of the AFM inter-nanomagnet coupling, makes the nanomagnets with corresponding anisotropy energy over-relaxed so that the magnetiza-tion curve (warming from 10 K) has a small dip at the same 40 K with respect to the reference curve. As for the aging effect shown in Figure 5, the key point is that the system is still relaxing at the base temperature 15 K during the additional waiting period t_w. For larger t_w, the system becomes more relaxed and the magnetization is a little smaller until a time $t \approx t_w$. However, the effect of the additional relaxation of t_w will finally disappear for $t \gg t_w$. Therefore, there is a peak for the rate of increasing the magnetization at a time $t \approx t_w$.

Compared with experiments and other theories. Sim-ilar FC and ZFC magnetization memory effects were observed in both spin (including super-spin) glass sys-tems and isolated nanomagnets, and similar ZFC mem-ory and aging effects in spin glass systems[13, 14, 15, 16, 17, 18, 22, 23]. Usually, memory effects in iso-lated nanomagnets were attributed to broad distribu-tion of relaxation times for different nanomagnets. The memory and aging effects in spin glass systems can be understood in terms of droplet model and hierar-chy model[15, 16, 17, 18]. For our systems the mag-netic anisotropy is uniaxial and the inter-spin interaction is uniformly AFM, and therefore our model, including inter-spin interaction, is distinguished from other ones for those systems[13, 14, 15, 16, 17, 18, 22, 23].

V. CONCLUSION

Using the dynamical spin Monte Carlo method, we in-vestigate various nonequilibrium dynamical magnetiza-tion behaviors of the representative systems (finite two-dimensional lattices) composed of antiferromagnetically-coupled sub-10nm grained nanomagnets with large uni-

axial anisotropy. In each of such systems of the nanomagnets with the same easy axis, we find both ZFC and FC magnetization memory effects over both time and temperature and the magnetization aging effect, which partly appeared otherwise in different spin (or super-spin) glass systems and interacting nanoparticles. We explain these interesting dynamical effects in a unified way in terms of the continuously-distributed relaxation times of the interacting nanomagnets due to their large anisotropy energies in the actual media.

Acknowledgments

[1] S.D. Bader, Rev. Mod. Phys. 78 (2006) 1.
[2] S. Krause, L. Berbil-Bautista, G. Herzog, M. Bode, R. Wiesendanger, Science 317 (2007) 1537.
[3] S. Bertaina, S. Gambarelli, T. Mitra, B. Tsukerblat, A. Mueller, B. Barbara, Nature 453 (2008) 203.
[4] M.N. Leuenberger, D. Loss, Nature 410 (2001) 789.
[5] L. Bogani, W. Wernsdorfer, Nat. Mater. 7 (2008) 179.
[6] D. Gatteschi, R. Sessoli, J. Villain, Molecular nanomagnets, Oxford University Press 2006.
[7] W. Wernsdorfer, N. Aliaga-Alcalde, D.N. Hendrickson, G. Christou, Nature 416 (2002) 406.
[8] W. Wernsdorfer, R. Sessoli, Science 284 (1999) 133.
[9] S. Hill, R.S. Edwards, N. Aliaga-Alcalde, G. Christou, Science 302 (2003) 1015.
[10] C. Schlegel, J. van Slageren, M. Manoli, E.K. Brechin, M. Dressel, Phys. Rev. Lett. 101 (2008) 147203.
[11] L. Neel, Ann. Geophys. 5 (1949) 99.
[12] W. Wernsdorfer, E.B. Orozco, K. Hasselbach, A. Benoit, B. Barbara, N. Demoncy, A. Loiseau, H. Pascard, D. Mailly, Phys. Rev. Lett. 78 (1997) 1791.
[13] T. Jonsson, J. Mattsson, C. Djurberg, F.A. Khan, P. Nordblad, P. Svedlindh, Phys. Rev. Lett. 75 (1995) 4138.
[14] M. Sasaki, P.E. Jonsson, H. Takayama, H. Mamiya, Phys. Rev. B 71 (2005) 104405.

[15] L. Lundgren, P. Svedlindh, P. Nordblad, O. Beckman, Phys. Rev. Lett. 51 (1983) 911.
[16] D.S. Fisher, D.A. Huse, Phys. Rev. B 38 (1988) 373; 38 (1988) 386.
[17] K. Jonason, E. Vincent, J. Hammann, J.P. Bouchaud, P. Nordblad, Phys. Rev. Lett. 81 (1998) 3243.
[18] F. Lefloch et al, Europhys. Lett. 18 (1992) 647.
[19] T. Thomson, L. Abelmann, H. Groenland, 'Magnetic data storage: past, present and future', in: Magnetic nanostructures in modern technology, edited by B. Azzerboni et al, Springer Dordrecht 2008, Pages 237-306.
[20] Y. Li and B.G. Liu, Phys. Rev. B 73 (2006) 174418; Phys. Rev. Lett. 96 (2006) 217201.
[21] T.A. Witten, L.M. Sander, Phys. Rev. Lett. 47 (1981) 1400.
[22] Y. Sun, M.B. Salamon, K. Garnier, R. S. Averback, Phys. Rev. Lett. 91 (2003) 167206.
[23] R.K. Zheng, H. Gu, B. Xu, X.X. Zhang, Phys. Rev. B 72 (2005) 014416.
[24] S. Sahoo, O. Petracic, W. Kleemann, P. Nordblad, S. Cardoso, P.P. Freitas, Phys. Rev. B 67 (2003) 214422.
[25] M. Osth, D. Herisson, P. Nordblad, J.A. De Toro, J. M. Riveiro, J. Magn. Magn. Mater. 313 (2007) 373.